Supernova Remnants: Cosmic-ray Accelerators in the Milky Way

Tülün Ergin, TÜBİTAK Uzay

Outline

- Cosmic Ray Origin
- Gamma and X-Rays
  - Production Processes
  - Detection Instruments
- Supernova Remnants
  - Definition and General Classes
  - Gamma-ray and X-ray Emission Mechanisms
- Example Studies
  - Multi-waveband Modeling of Cas A
  - Hadronic Emission and Recombining Plasma in 3C 391
- Conclusion

Non-thermal Radiation

- Particle radiation:
  - Solar Energetic Particles: protons, electrons, heavy ions
  - Neutrinos
  - Cosmic Rays (CRs): protons (86%), nuclei, electrons)
- Photon Radiations:
  - Radio emission (by cosmic ray electrons)
  - X-rays and gamma rays (by cosmic ray electrons, protons, and ions)

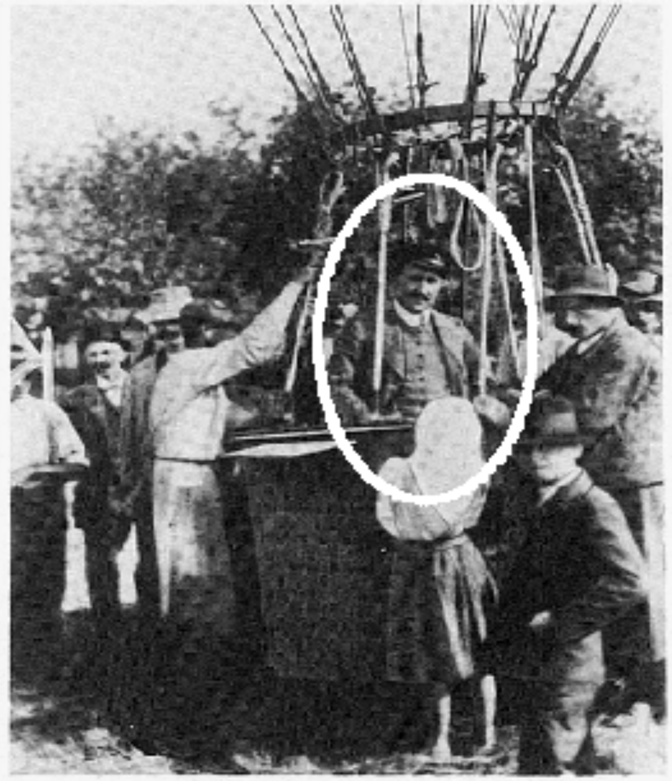

Victor F. Hess

Measurements of ionization intensity during balloon flights (1912).

Nobel prize 1936

The Origin of CRs

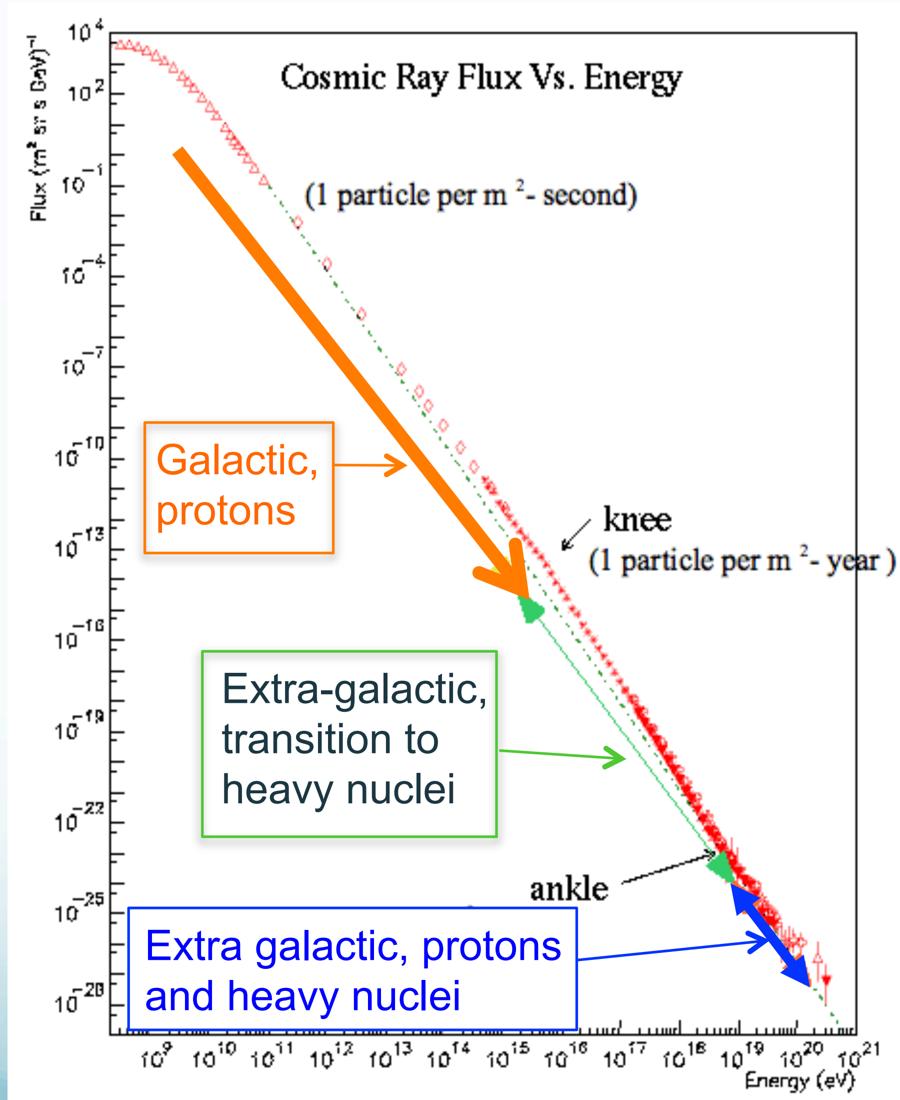

Shock-wave acceleration in supernova remnants (SNRs) ?

The Origin of Galactic CRs

- Supernova explosion
  - 10 billion times brighter than the Sun
  - **Type-Ia: energy = thermonuclear fusion**
    - E = 2 MeV/nucleon
    - Total energy: 10^{51} erg
  - **Type II, Ib, Ic : energy = gravity**
    - E = 200 MeV/nucleon
    - Total energy: 10^{53} erg
    - Kinetic energy: 10^{51} erg

- Kinetic energy (~10^{51} erg) released as expanding stellar material (ejecta, ~$M_{\odot}$) creates an SNR
  - Sources of (heavy) elements
  - Sources of kinetic energy in the ISM
  - **Sources of cosmic rays**

Supernova Explosion

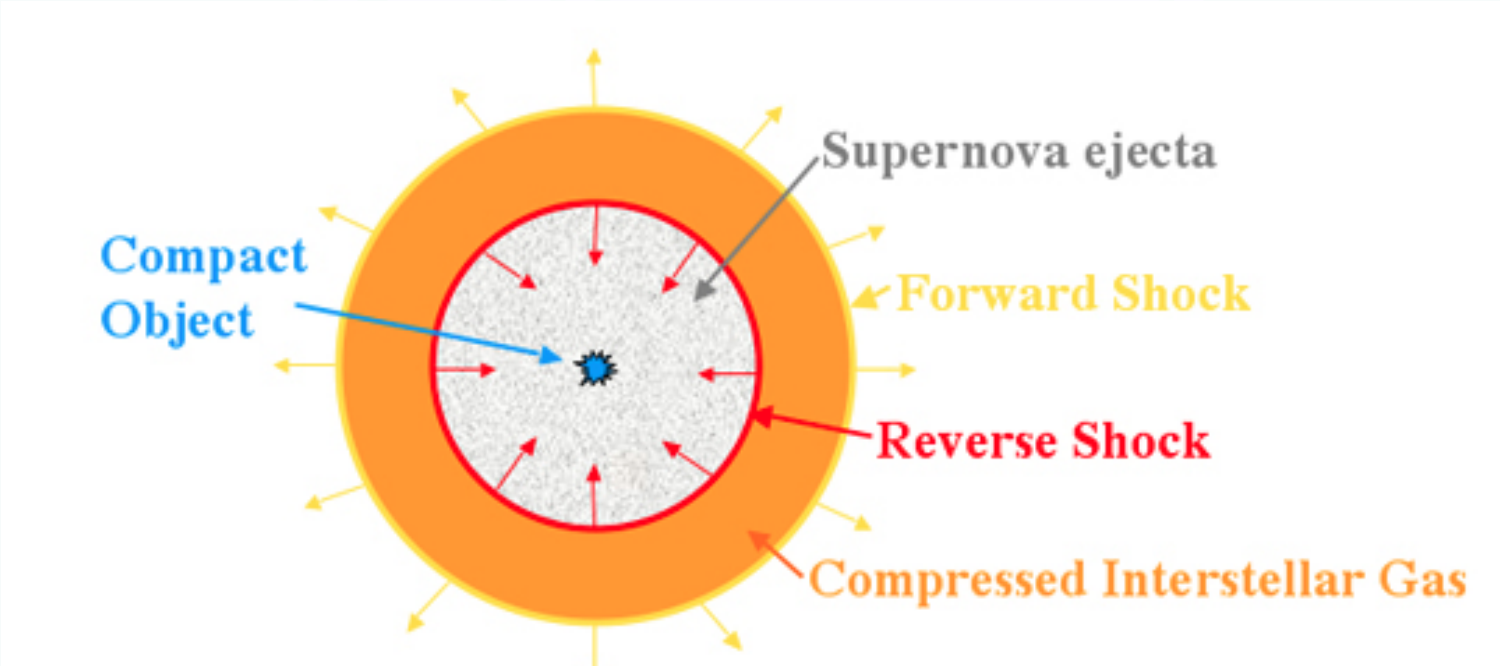

A forward and a reverse shock are created when the supernova shock wave interacts with the interstellar medium (ISM). The forward shock continues to expand into the ISM, the reverse shock travels back into the freely expanding supernova ejecta.

Finding CR Sources

- Protons, Nuclei
  - Deflected by galactic/intergalactic magnetic fields → Isotropic distribution
  - Exception: CR with energies above the “ankle” → Auger project
- Neutrinos
  - Direct signature from hadronic interactions, and not absorbed by intergalactic IR fields
  - Weak emission → difficult to detect
- Gamma & X-rays
  - Not deflected → Point back to its source

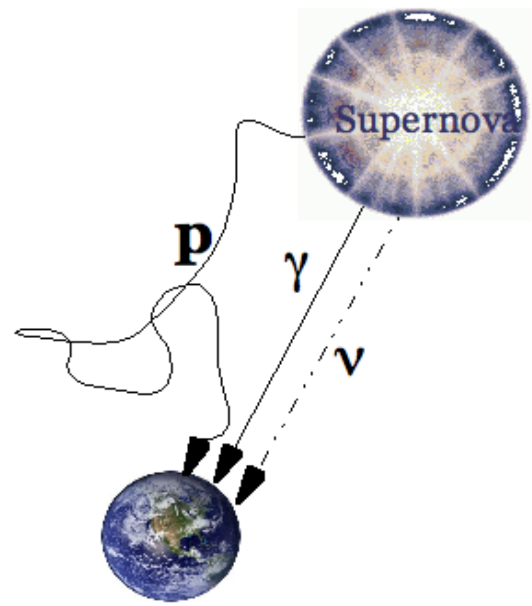

Gamma-ray Production

- Charged particles in strong electromagnetic fields
  - Bremsstrahlung (Leptonic)
    - VHE charged particles accelerated in electric field
  - Synchrotron radiation
    - VHE electrons moving in strong magnetic field

- Inverse Compton (IC) scattering (Leptonic)
  - Up-scattering of photons of lower energy through collision with VHE particles

- Decays and annihilation
  - Pair annihilation
    - Particle + Anti-Particle → $\gamma + \gamma$
  - Pion production and decay (Hadronic)
    - Proton + Matter → π° → $\gamma + \gamma$

X-ray Production

- Thermal bremsstrahlung
  - Accompanied by emission lines
- High-energy electrons in SNRs produce X-rays via two mechanisms
  - Non-thermal bremsstrahlung
  - Synchrotron emission

Ground-based Observatories of IACTs*

* Imaging Atmospheric Cherenkov Telescopes
** Decommissioned

VERITAS

Geographic Location: 31° 40´ North, 110° 57´ West, Altitude: 1268 masl.
Energy range: 100 GeV < E < 10 TeV
Sensitivity: ~1% of the flux of the Crab Nebula detected in 25 hours

TeV Sources 2015

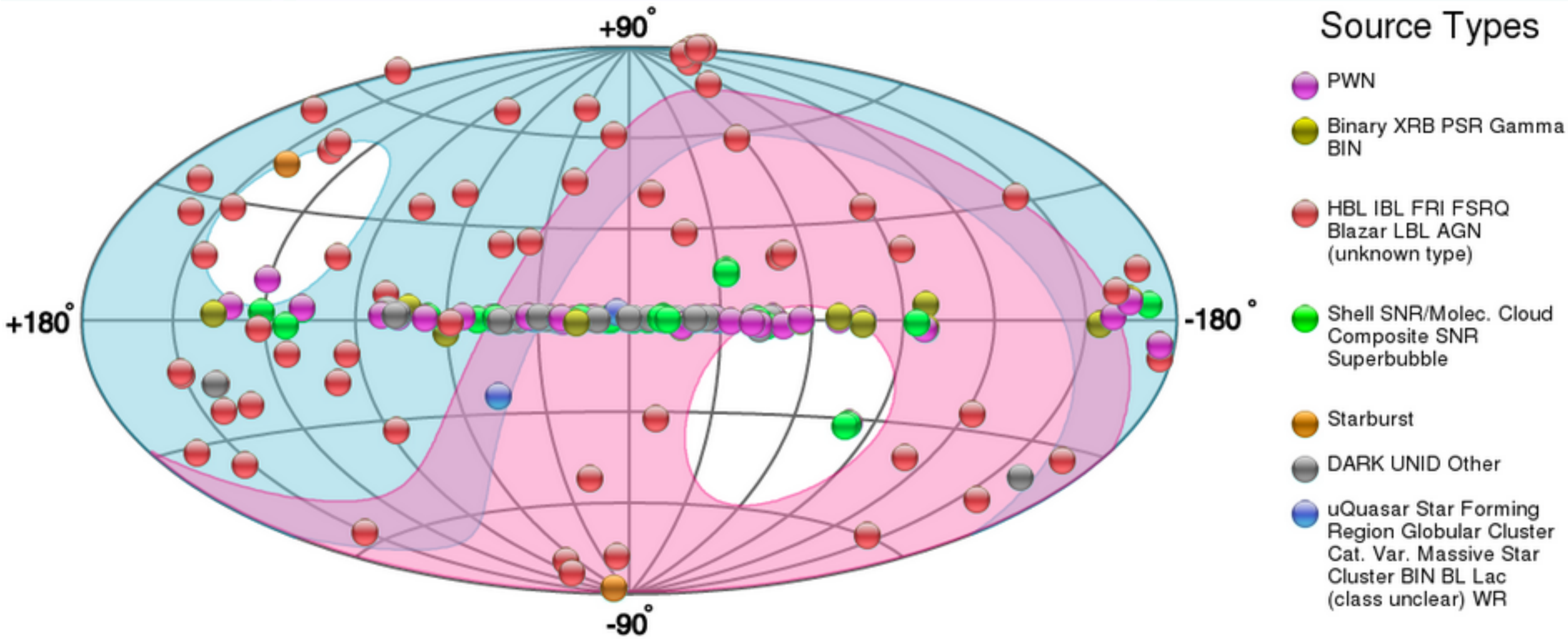

http://tevcat.uchicago.edu/

As of October 2015:

195 sources in total. Detected farthest distance object at z=0.944.

Fermi Gamma-ray Space Telescope

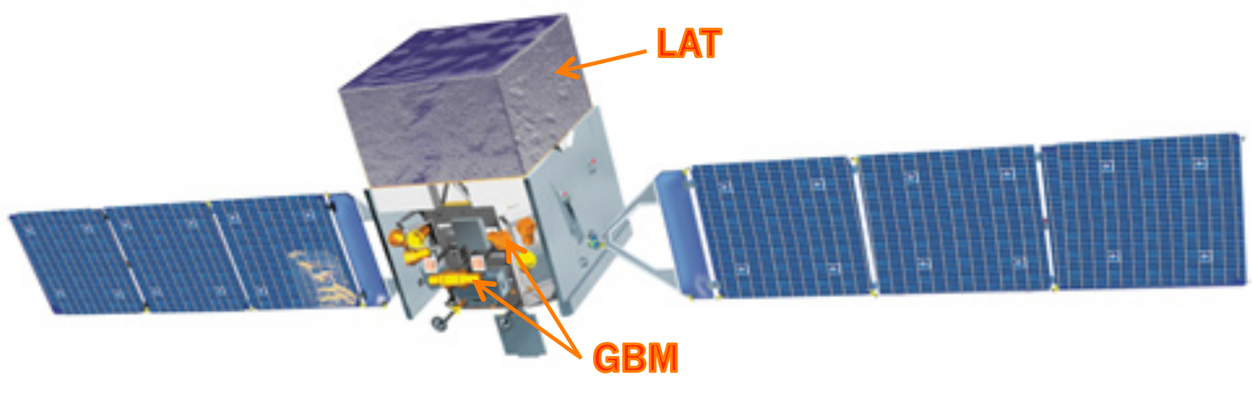

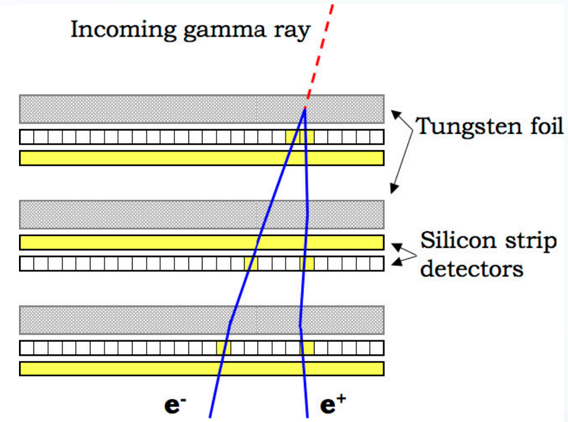

- Launched on June 11, 2008
- Two instruments
  - Large Area Telescope (LAT)
    - 20 MeV – 300 GeV
  - Gamma-ray Burst Monitor (GBM)
    - 10 keV – 25 MeV

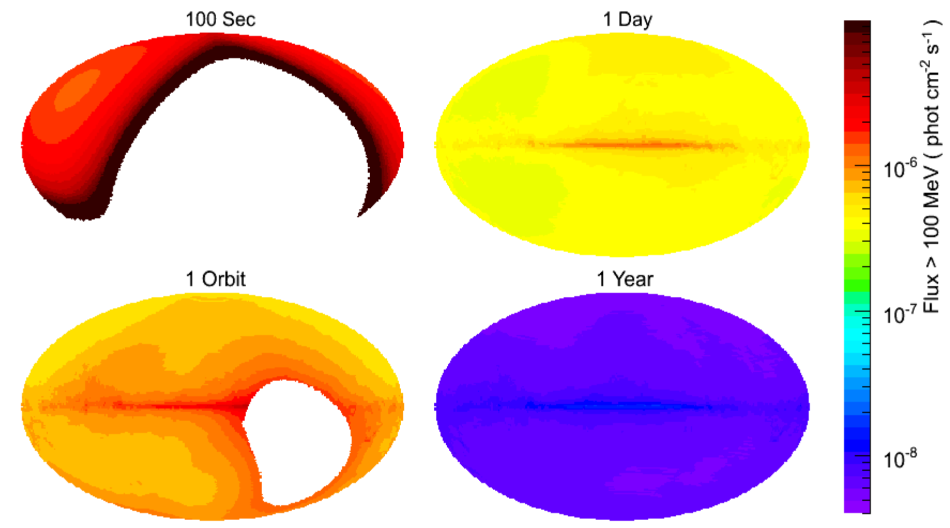

Atwood et al. (arXiv:0902.1089)

Sensitivity to Point Sources

First SNRs Detected by Fermi-LAT

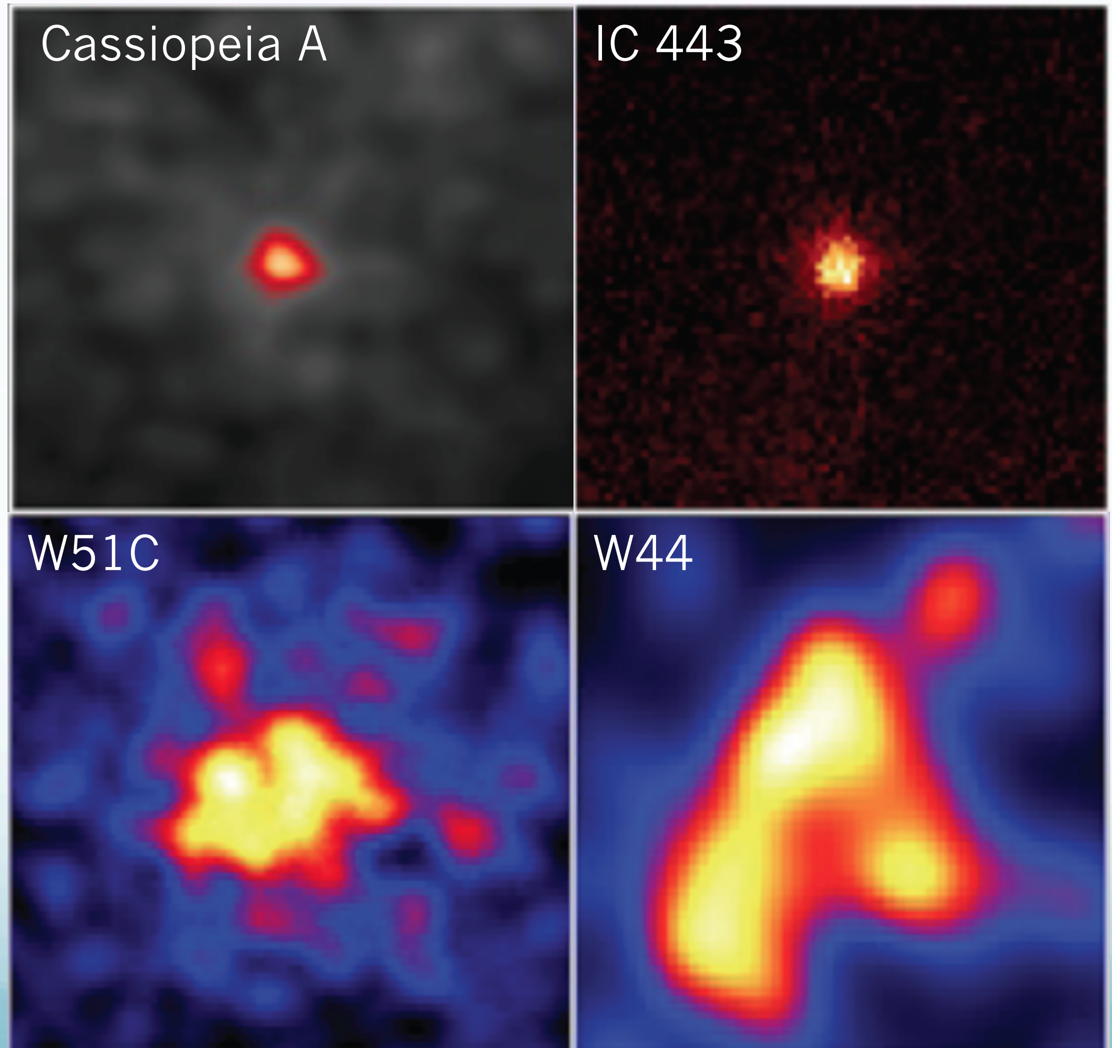

X-ray Satellites

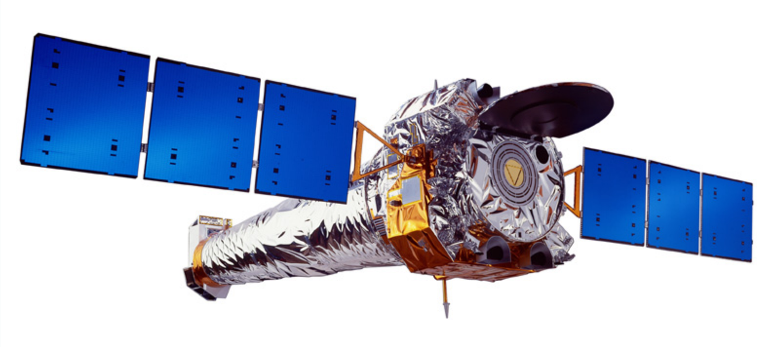

- **Chandra**
  - Launched on July, 23 1999
  - Energy Range: 0.1 – 10 keV
  - Instruments on board
    - High Resolution Camera (HRC)
    - Advanced CCD Imaging Spectrometer (ACIS)
    - High Resolution Spectrometers (HETGS & LETGS)

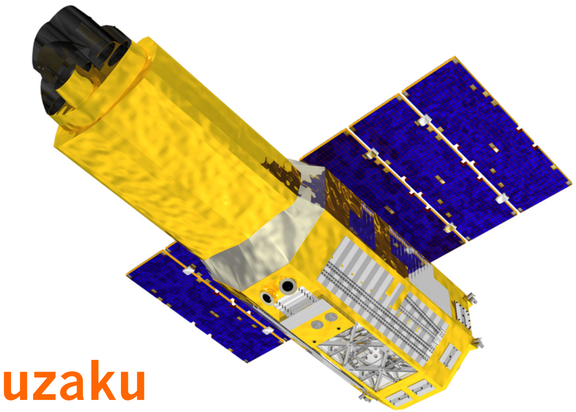

- **Suzaku**
  - Launched on July, 10 2005
  - Energy Range: 0.3 – 600 keV
  - High resolution spectroscopy
  - Instruments on board
    - X-ray Spectrometer (XRS) (shut down Aug, 8 2005)
    - X-ray Imaging Spectrometer (XIS)
    - Hard X-ray Detector (HXD)

The SNR Classification

- According to Origin
  - Core-collapse or Type-Ia SNR
- According to Radio & X-ray Morphology

SNR	Shell-like	Center-like
Shell-type	yes	no
Plerion-type	no	yes
Composite-type	yes	yes
Mixed Morphology (Radio)	yes	no
Mixed Morphology (X-rays)	no	yes

Why do we study SNRs?

- SNR interactions with dense clouds to study cosmic rays
  - Type & maximum energy of emitting population (electrons or ions)
  - Propagation / diffusion of cosmic rays in interstellar medium
- Plerion science
  - Measure magnetic field strength
  - Study cooling breaks and cut-offs in broad-band spectra
- Broad-band spectral and morphological studies
  - Spatially resolved properties of non-thermal populations
  - Common population of objects across GeV / TeV

Shell-type SNRs

- No electrons supplied by the pulsar wind
- Shells of the remnants possibly hadron or electron acceleration sites
  - Gamma rays from hadrons through $\pi^{\circ} \rightarrow 2\gamma$
  - Gamma rays from electrons through IC scattering
- Gamma-ray signal from shell regions may give hints for hadron acceleration
  - Signal could be enhanced by shell interacting with nearby molecular clouds

Cassiopeia A: A Young Shell-type Remnant

- Born in 1680 in our Galaxy
- One of the brightest radio sources in the sky
- Angular size of 2'.5 in radius
  - Size of 2.34 pc at a distance of 3.4 (+0.3 –0.1) kpc
- Strong magnetic fields implied from X-ray variability on short timescales

VERITAS & Fermi View of Cas A

- Previously detected by HEGRA, MAGIC
- VERITAS detection of 8.3 σ in 22 hours
  - Spectral Index: $\Gamma = 2.61 \pm 0.24^{stat} \pm 0.2^{sys}$
  - Flux above 1 TeV: $(7.76 \pm 0.11) \times 10^{-13}$ cm^{-2} s^{-1} (3% of Crab Nebula flux)
- Fermi detection of ~12σ after 2-years of data taking
  - Is consistent with a point source (3'.5)
  - Pulsar? No sign for a cut-off as in many pulsar spectra
- Spectrum does not rule out leptonic models

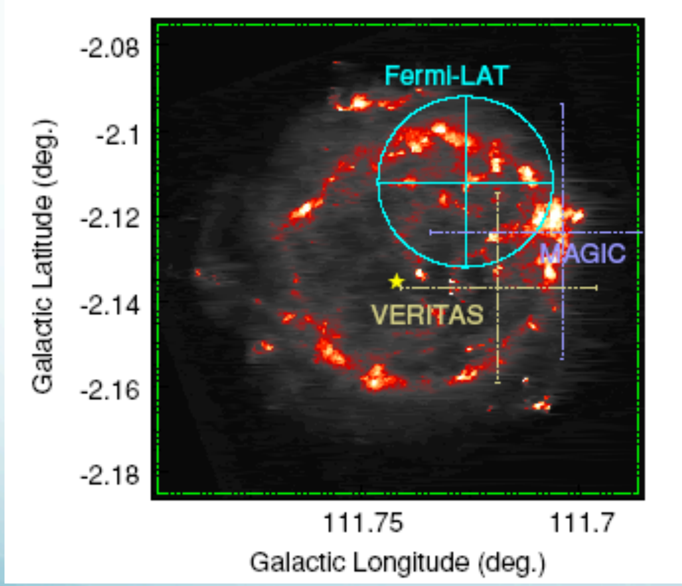

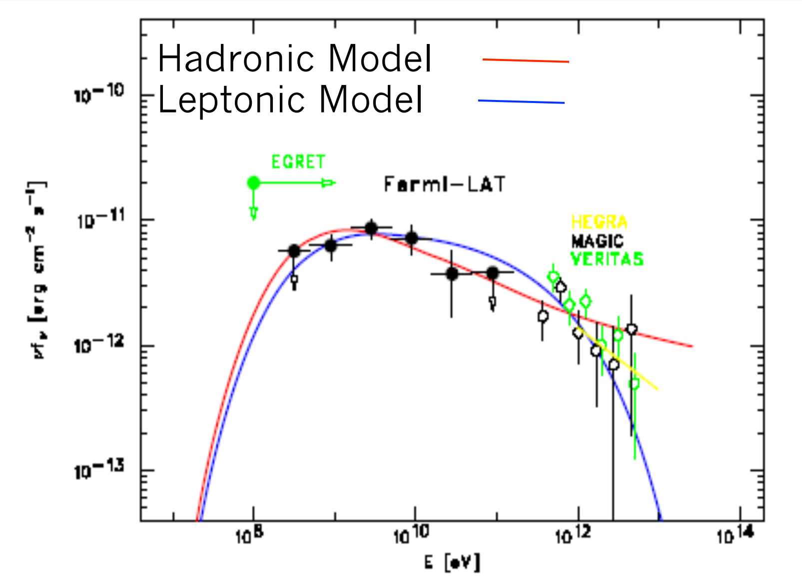

HEGRA: Aharonian, F. et al., A&A, 370,112 (2001),
MAGIC: Albert, J. et al.,A&A, 474,397 (2007),
VERITAS: Acciari, V.A. et al., ApJ, 698, L133 (2010).
Fermi-LAT: Abdo et al., ApJ, 710, L92 (2010).

Multi-wavelength Study of Cas A

How can we locate the origin of gamma rays based on the X-ray data of the shell of Cas A, and explain the GeV & TeV gamma-ray data in the context of both leptonic and hadronic scenario?

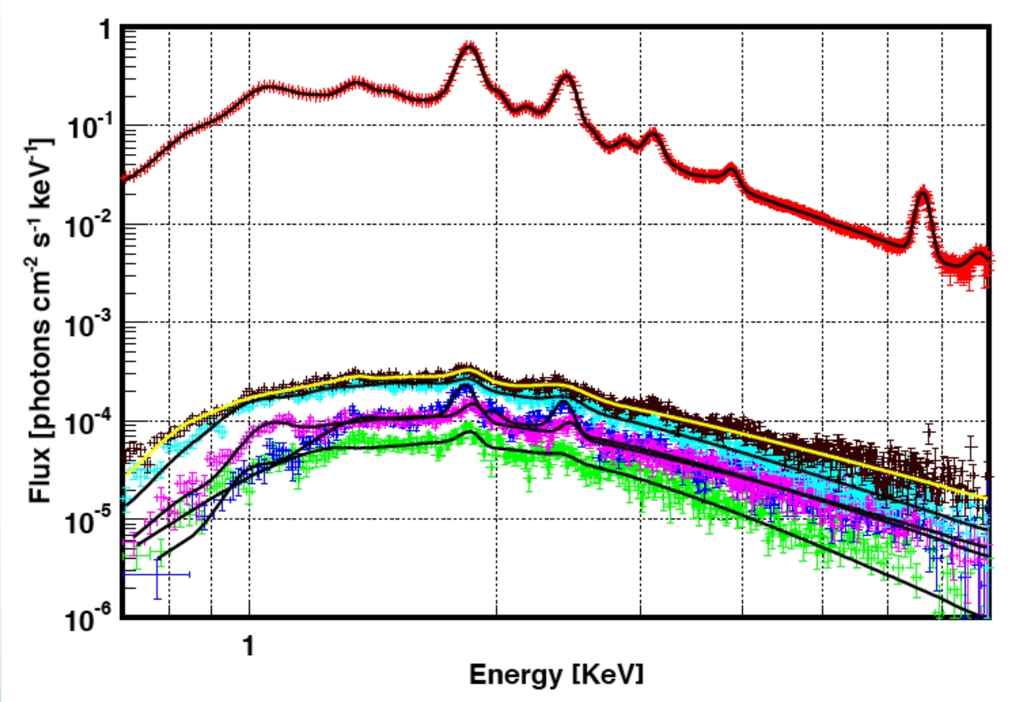

Saha, L., Ergin, T., Majumdar, P., Bozkurt, M., Ercan, E. (2014), A&A, 563, 88.

Selecting X-ray Regions on the Shell of Cas A

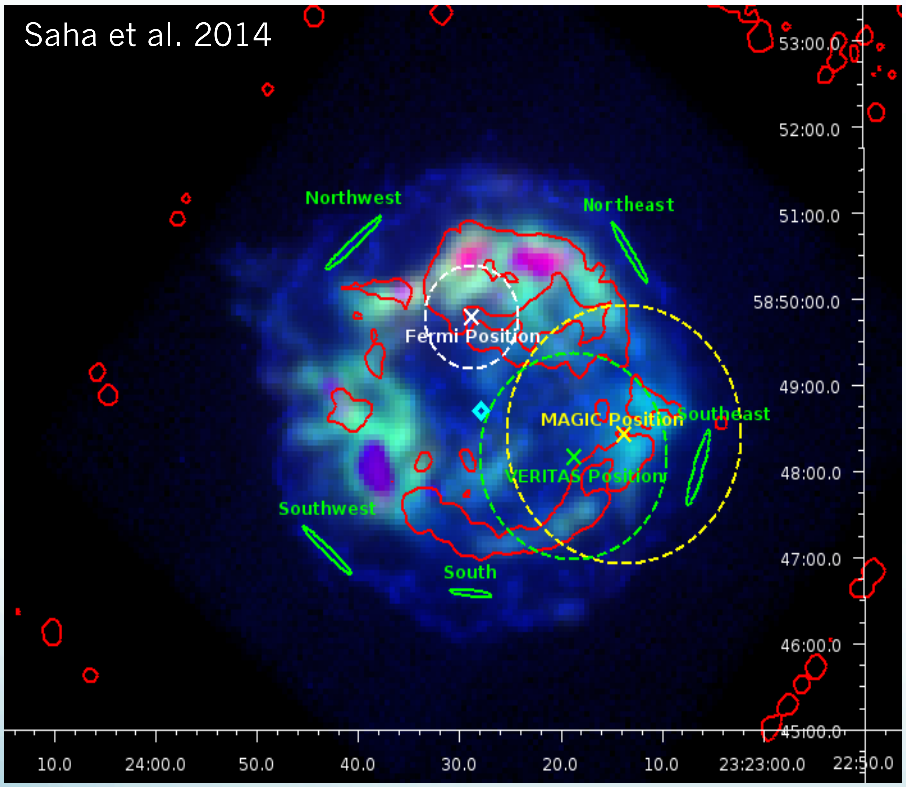

- The red, green, and blue color hues: The energy ranges of [0.7, 1.0], [1.0, 3.5], and [3.5, 8.0] keV, respectively.
- The green ellipses: selected S, SW, SE, NW, and NE regions
- The green and yellow crosses and dashed circles: The VERITAS and MAGIC locations and approximated location error circles.
- The white cross and dashed circle: The GeV gamma-ray emission best-fit location and the location error circle
- Cyan open diamond: The CCO location
- Red contours: The derived CO data from Spitzer-IRAC starting from a value of 0.4 MJy/sr and higher

Modeling the Synchrotron Emission for All Regions

- The fit synchrotron spectra and the observed best-fit X-ray spectra for the regions are shown by lines and stripes, respectively.

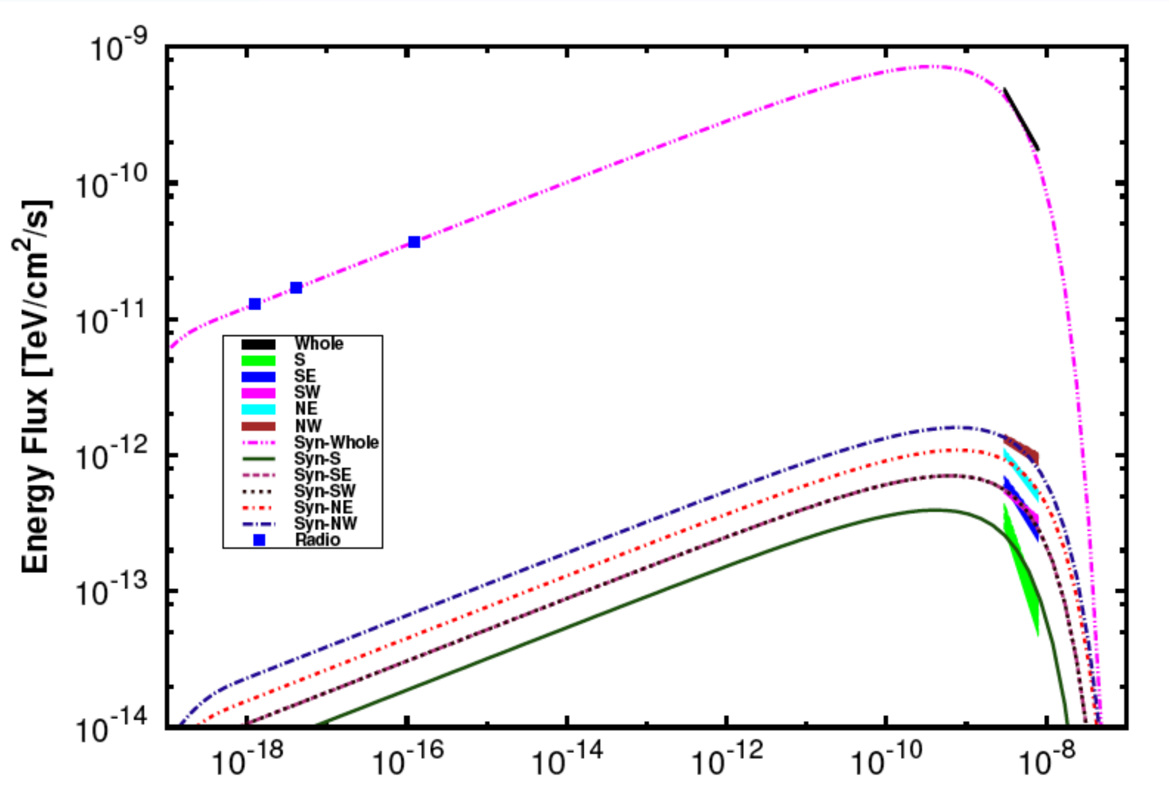

Saha et al. 2014

Region	Magnetic Field (B) [μG]
South	**250**
Southwest	**330**
Southeast	**330**
Northeast	**410**
Northwest	**510**

Modeling the Inverse Compton Emission

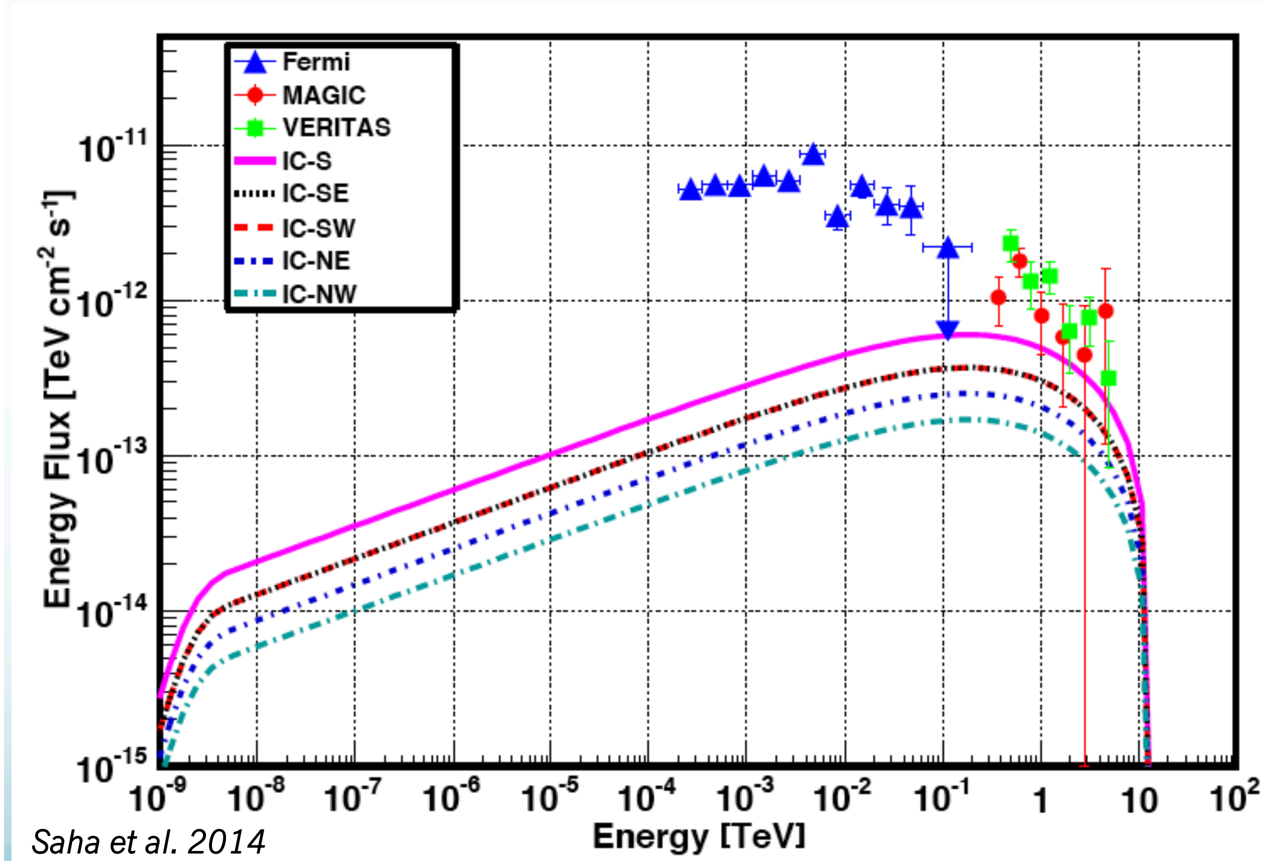

- If the shell region is dominated by strong magnetic field (e.g. 510 G), then the IC component of radiation is reduced.
- The TeV flux from the S region of the shell is higher than those from other regions of Cas A.

Modeling the Total Leptonic Emission for the S Region

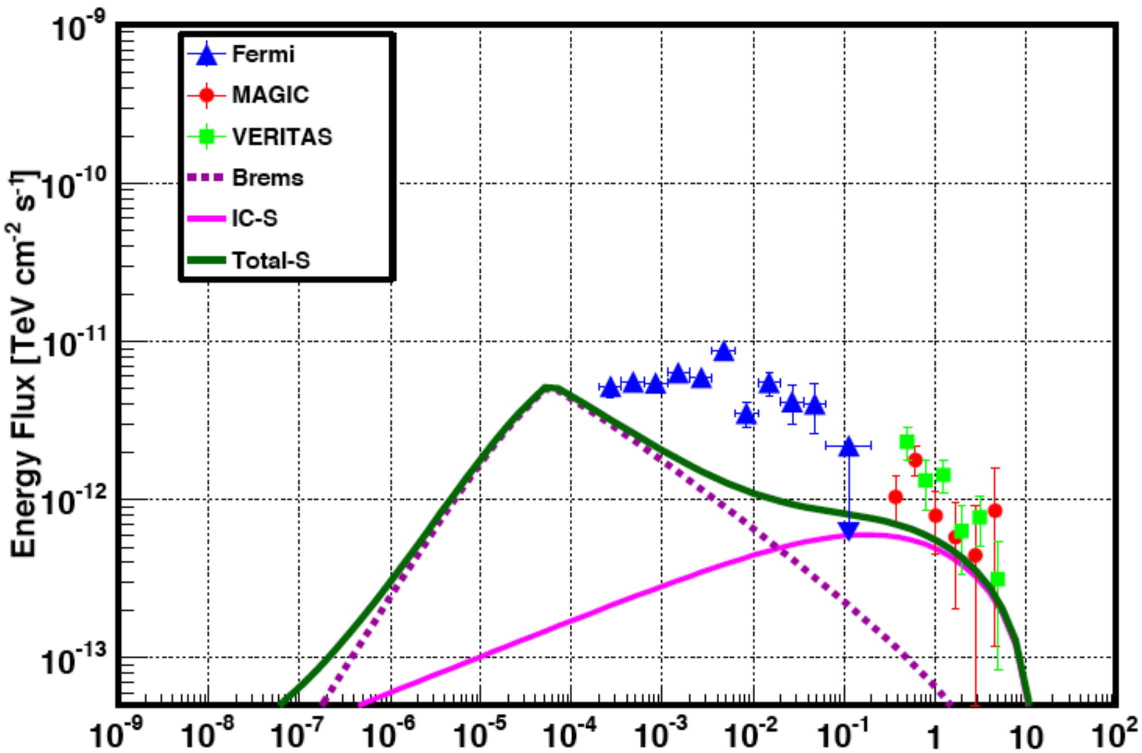

Saha et al. 2014

But the total leptonic model does not fit to the GeV gamma-ray data from Fermi-LAT!

- IC (solid line) and bremsstrahlung (dashed line) spectra are estimated for the whole remnant.
- Electron spectrum parameters are based on S region.
- Bremsstrahlung spectrum calculated for $n_H = 10$ cm^{-3}
- The thick solid line corresponds to total contribution to gamma rays from leptons (electron)
- The parameters for radio emitting electrons are $\alpha = 2.54$ and $\gamma_{max} = 3.2 \times 10^7$ (Lorenz fact. of cutoff energy)

The Lepto-hadronic Gamma-ray Emission Model

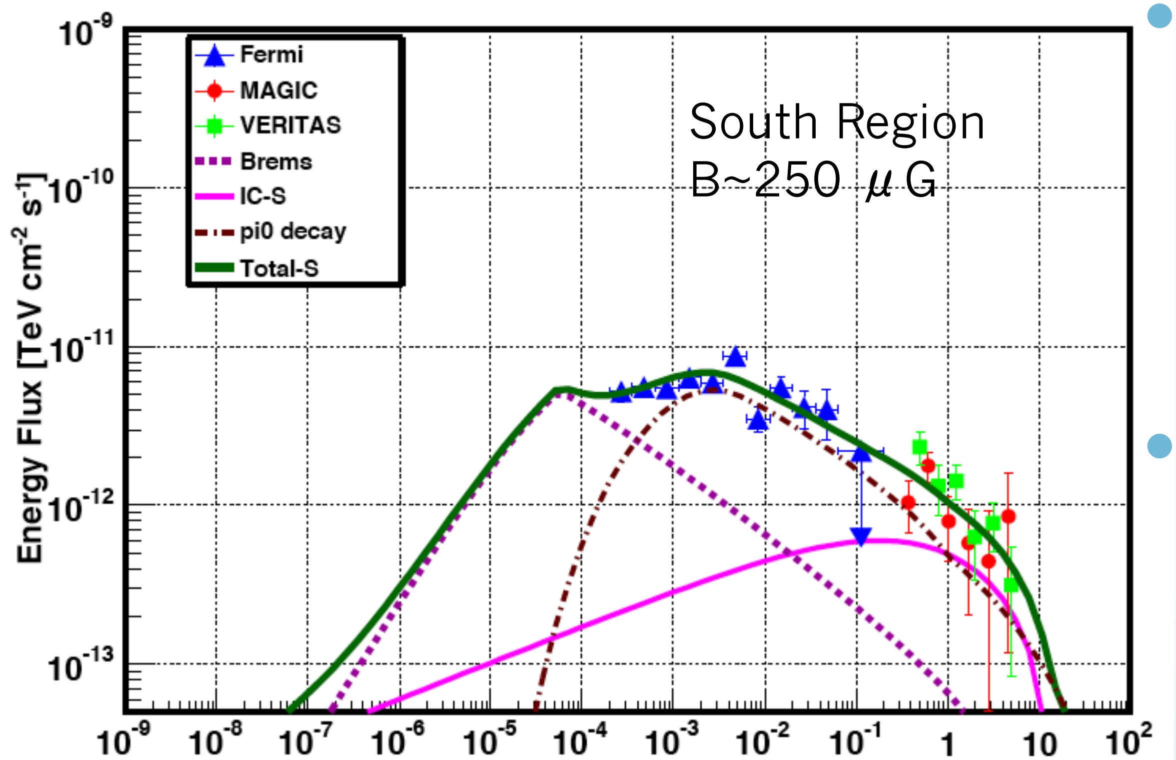

Saha et al. 2014

- Gamma-ray spectrum (thick solid line) of Cas A for combining both leptonic and hadronic contribution to the whole remnant data.
- The total energy of the charged particles is $W_e + W_p = 3.4 \times 10^{49}$ erg
  - Gives a conversion efficiency of supernova explosion energy to be < 2%

Model Fit Results

$$\frac{dN}{dE_p} = N_1\, E_p^{-\rho} \text{ for } E_p^{\min} \leq E_p < E_p^{\text{break}}$$
$$= N_2\, E_p^{-\beta} \exp\left(-\frac{E}{E_p^{\max}}\right) \text{ for } E_p^{\text{break}} \leq E_p,$$

Parameters	Set-I (hadronic)	Set-II (hadronic+leptonic)
ρ	2.05 ± 0.05	1.26 ± 0.2
β	2.36 ± 0.02	2.44 ± 0.03
$E_p^{\max}$ (TeV)	100	100
E_p^{break} (GeV)	17	17
Energy (W_p) (erg)	5.7×10^{49}	2.97×10^{49}
χ^2/d.o.f.	2.5	1.8

Saha et al. 2014

Magnetic fields might be amplified through two ways

- Through magneto-hydrodynamic waves generated by cosmic rays (Bell & Lucek 2001; Bell 2004)
- From the effect of turbulent density fluctuations on the propagating hydrodynamic shock waves (Giacalone & Jokipii 2007).

But too low conversion efficiency to cosmic rays (2%)

- The cosmic ray streaming energy not sufficient enough to be transferred to the magnetic fields resulting magnetic amplification!
- The magnetic field amplification in the down-stream of shocks of Cas A might be due to presence of turbulence

Mixed-Morphology (MM) SNRs

- Different Morphology in X-ray and radio band: Thermal X-rays from the central region and radio emission from the shell.
- 10% of all Galactic SNRs and 25% of all X-ray detected Galactic SNRs are MM-type.
- First detected SNRs by Fermi-LAT were mostly middle-aged MM-type SNRs: W44, IC 443, W28, W49B, and W51C.
  - Interactions of these MM-type SNRs with molecular clouds (MC) proven by the 1720 MHz OH masers.
  - MM SNRs interacting with MC are targets for detecting gamma rays of hadronic origin.
    - Provides clear evidence for these SNRs to be sites of proton acceleration.

Origin of MM-type SNRs

- Interactions with MC hint associations with star forming regions (SFRs)
  - SFRs contain massive stars with strong stellar winds surrounded by circumstellar matter (CSM)
  - Possibly these massive stars are the progenitors of MM-type remnants.
- When the supernova blast wave breaks out of the CSM into the ISM, the particle acceleration increases.

3C 391: A Middle-aged MM SNR

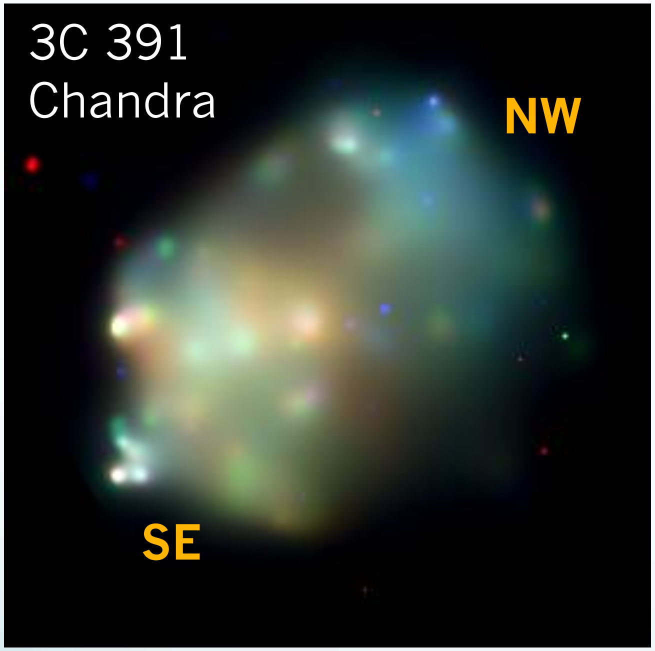

- A MM-type SNR at a distance between 7.2 and 11.4 kpc
- A partial radio shell of 5' diameter with breakout morphology
  - Intensity of the radio emission in the shell rises in the bright northwest rim (NW) and drops and vanishes toward the southeast rim (SE).
- Observed in X-rays by Einstein, ROSAT, Chandra, ASCA
  - Revealed brightest X-ray peak interior to the weak SE rim and a fainter one in the interior of the bright NW radio shell.
- Two OH masers at 1720 MHz coincident with the SE and NE rim of 3C 391.
  - First clear evidence for 3C 391 interacting with an MC.

Fermi-LAT View of 3C 391

- Listed in the 2nd & 3rd Fermi-LAT catalogs as a point-like source
  - 2FGL J1849.3–0055 (3FGL J2323.4+5849)
- Castro & Slane (2010) reported
  - $\sim 12\sigma$ detection
  - The peak of the significance map was shifted 4' away from the NW edge of the radio shell.
  - Power-law model spectral index: $\Gamma = -2.33 \pm 0.11$
  - Integrated flux: F(0.1–100 GeV) = $(1.58 \pm 0.26) \times 10^{-7}$ ph cm^{-2} s^{-1}
- TeV observation results from H.E.S.S.
  - Integral flux upper limit (at the 95% CL) = 0.8 Crab Nebula flux units

Fermi-LAT Analysis Results

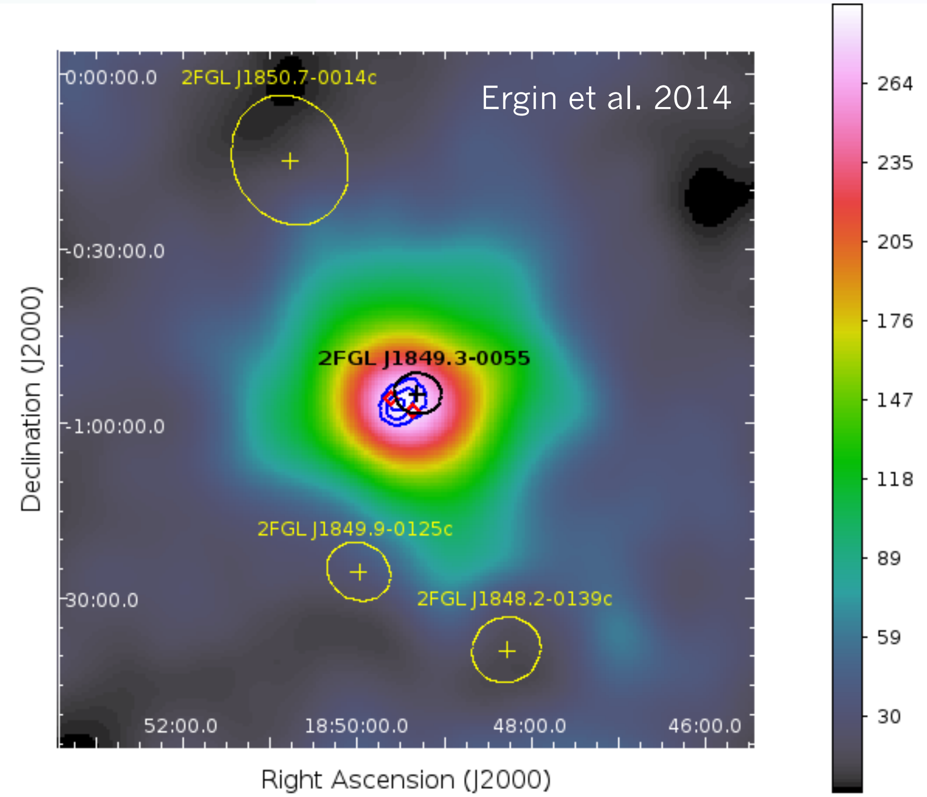

Test statistics (TS): Larger TS values indicate that the null hypothesis (maximum likelihood value for a model without an additional source) is incorrect. Source significance is approximately the square-root of the TS value.

- 5 years of Fermi-LAT data
- $\sim 18\sigma$ signal detection
- Motivation:
  - Is the gamma-ray emission hadronic in origin due to the interaction between the SNR & MC?
    - Can we obtain information about the parent proton spectrum?
  - Is 3C 391 extended in gamma rays?
  - Is the gamma-ray emission form 3C 391 variable in time?

Ergin, T., Sezer, A., Saha, L., Majumdar, P., Chatterjee, A., Bayirli, A., Ercan, E. N. (2014), ApJ, 790, 65.

Gamma-ray Light Curve

- Checked data from the circular region of 1° around the best-fit position
- Fitting 3C 391 spectrum assuming standard spectrum of a pulsar (PLEC)
- Best-fit cutoff energy found to be 28.80 ± 6.73 GeV
  - An order of magnitude away from the range of typical pulsar cutoff energies
- Fitting the flux points to a straight line yields a X^2/dof of ~1.25 assuming a PLEC type spectrum for 3C 391
  - No long term variability observed for 3C 391

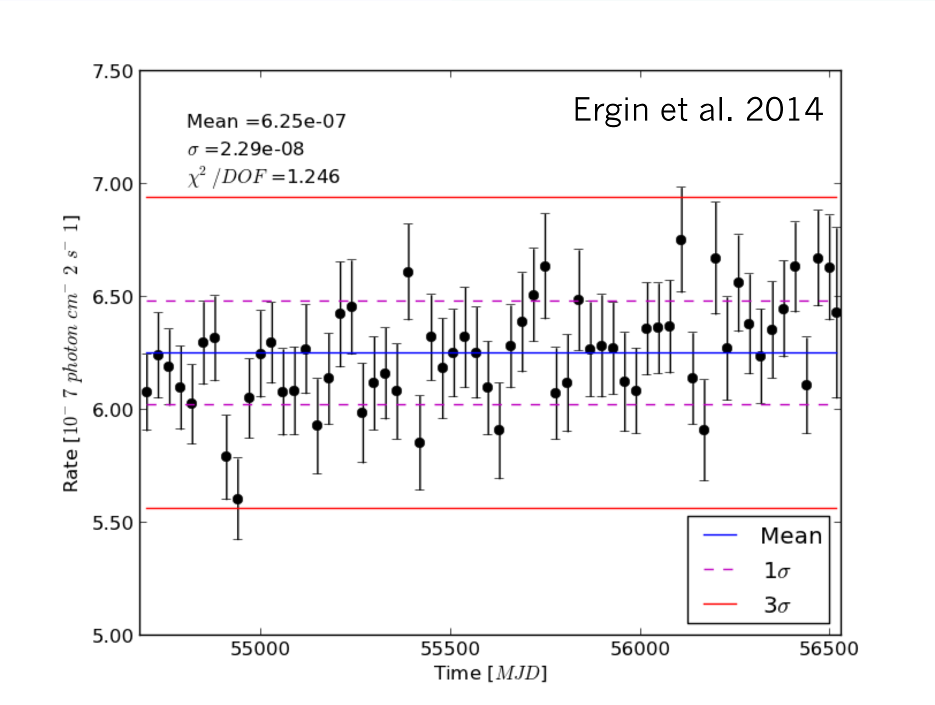

Molecular Map around 3C 391

Top from left: [$-$*50,0], [0,15]*,[15,35]; Bottom from left: [35,60], [60,90], [90,120] km s^{-1}
For all maps, the range for W_{CO} is fixed between 0 and 92.8 K km s^{-1}.

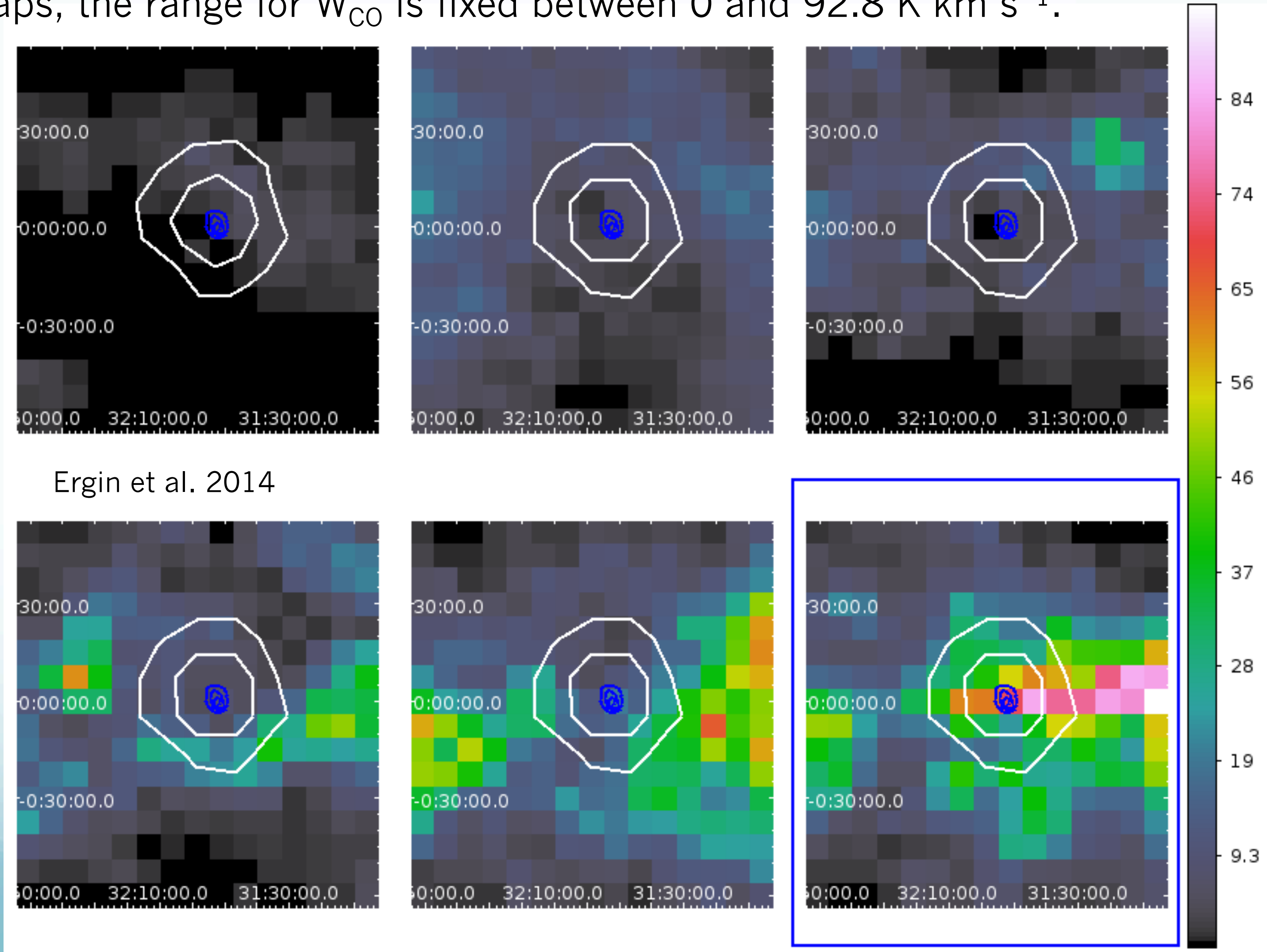

Modeling the Gamma-ray Spectrum

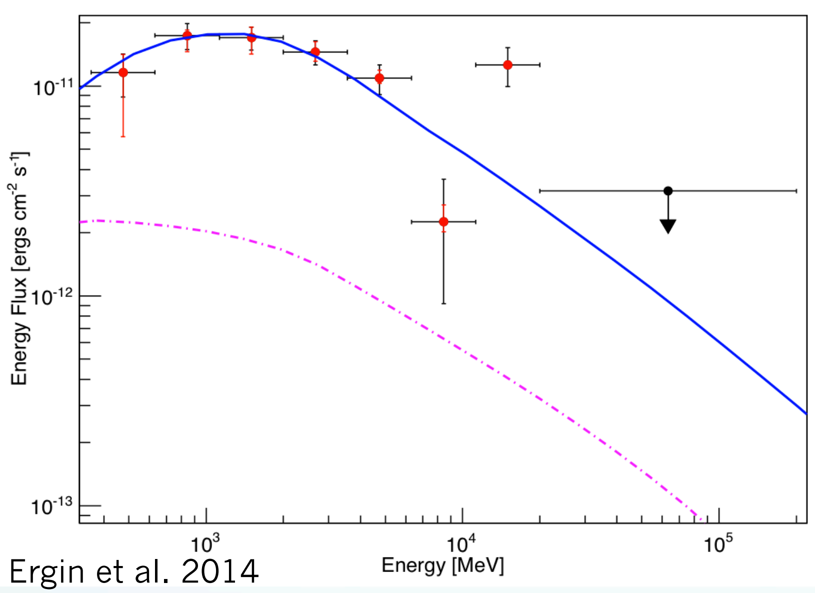

Ergin et al. 2014

Spectral Model	Photon Flux (10^{-8} photon cm^{-2} s^{-1})	Γ_1	Γ_2	E_b (MeV)	TS
PL	15.0 ± 1.7	2.30 ± 0.03	…	…	337
LP	7.14 ± 0.34	2.27 ± 0.04	0.15 ± 0.45	2430	337
BPL	4.89 ± 0.57	1.28 ± 0.50	2.50 ± 0.04	1060	338

- Red filled circles are spectral data points with black statistical errors and red systematic errors.
- Blue line: the fit to the spectrum from the decay of π° decay using a BPL distribution of protons. Dashed dotted line is the Bremsstrahlung model.
- Different spectral shapes tested
  - Best-fit TS value of 338 for BPL
- Total energy of protons

  $W_p \sim 5.8 \times 10^{48}$ erg x (387 cm^{-3} /n_H)

  n_H : Effective gas number density for p-p collision

The Proton Spectrum

- The luminosity of 3C 391 is L = 1.34×10^{36} erg s^{-1}
  - In the same ballpark with other middle-aged MM SNRs detected by Fermi-LAT, e.g. IC443, W44, W51C, etc.

- Spectral break at ~ 12 GeV in the parent BPL proton spectrum with index parameters of α = 2.48 and β = 3.0
  - Particles are escaping from the acceleration site to the rarefied ISM from the shell broken-out from the dense MC
    - TeV particles can only be confined during early stages of the SNR → But 3C 391 middle-aged SNR
    - Interaction between MC and SNR can speed up particle escape

- Assuming the BPL spectrum of protons without any spectral cut-off
  - The differential flux of gamma rays at 1 TeV ~ 0.06% of Crab nebula flux
  - TeV observations of 3C 391 with the upcoming Cherenkov Telescope Array (CTA) will provide more robust constraints of the various parameters of the input proton spectrum.

X-ray Plasma in SNRs

- Ionizing Plasma (IP): Found in young SNRs and are created by the shocks
  - The thermal energy of electrons (kT_e) > the ionization energy (kT_z).
- The plasma gradually reaches collisional ionization equilibrium (CIE)
  - An equilibrium state between recombination and ionization is established ($kT_e = kT_z$).

Recombining Plasma (RP) in SNRs

- The X-ray studies of ASCA on six MM SNRs revealed the existence of recombining plasma for IC443 and W49B ($kT_z > kT_e$).
- *Suzaku* has discovered strong radiative recombination continuum (RRC) features from six MM SNRs
  - IC443
  - W49B
  - G359.1-0.5
  - W28
  - W44
  - G346.6-0.2

What is the Origin of RP?

- Thermal Conduction: When the hot ejecta inside the SNR interior, which is in the form of normal IP or CIE plasma, encounters cold MC, the electron energy will be transferred to the MC by thermal conduction and the electron temperature falls rapidly. This condition then forms the RP.
- Adiabatic Cooling: If the CSM surrounding a progenitor is dense enough, CIE plasma will be formed at the early stages of the evolution of an SNR. When the blast wave breaks out of the dense CSM and expands rapidly into the rarefied ISM, the electron temperature drops due to the fast cooling by adiabatic expansion, which results in RP.

Analysis of 3C 391 Suzaku Data

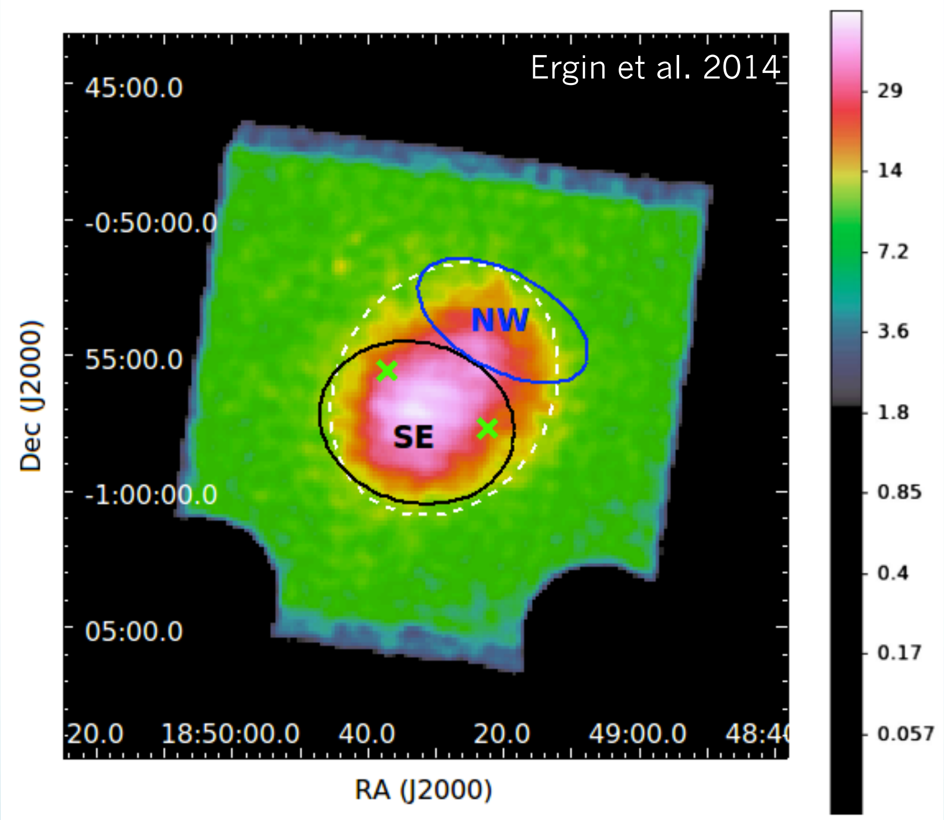

- Data taken by Suzaku (XIS) on October 22, 2010
- Exposure Time 99.4 ks
- Selected 3 signal regions
  - The whole SNR and the NW and SE regions of the SNR.
- The background for 3C 391 is a combination of
  - The non-X-ray background (NXB),
  - The Cosmic X-ray background (CXB) emission,
  - The Galactic ridge X-ray emission (GRXE).

Suzaku Spectral Fitting

- First Model: An absorbed (wabs in xspec) VNEI model for a non-equilibrium ionization (NEI) collisional plasma with variable abundances
  - NH, kT_e, n_et, and the abundances of Mg, Si, and S were free parameters.
  - The other elemental abundances were fixed to their solar values.
- The best reduced X^2/dof value of 1.44 for 1.0–5.0 keV

Suzaku Spectral Fitting

- Does the X-ray continuum comes from thermal bremsstrahlung or from RP?
  - There are residuals at ~2.0 keV and at ~2.6 keV.
  - Added two Gaussian components to the VNEI model corresponding to H-like (Lyα) lines of Si and S (indicators of highly ionized plasma)
  - We added the RP model of H-like Si (2.666 keV) and S (3.482 keV).
  - Also found Al K-shell emission at ~1.58 keV
- Adding Lyα lines and RP components the χ^2/dof value improved to 1.2
- Using *Suzaku* data we discovered RP in 3C 391.
- The final electron temperature for the whole remnant is cooler than the initial electron temperature

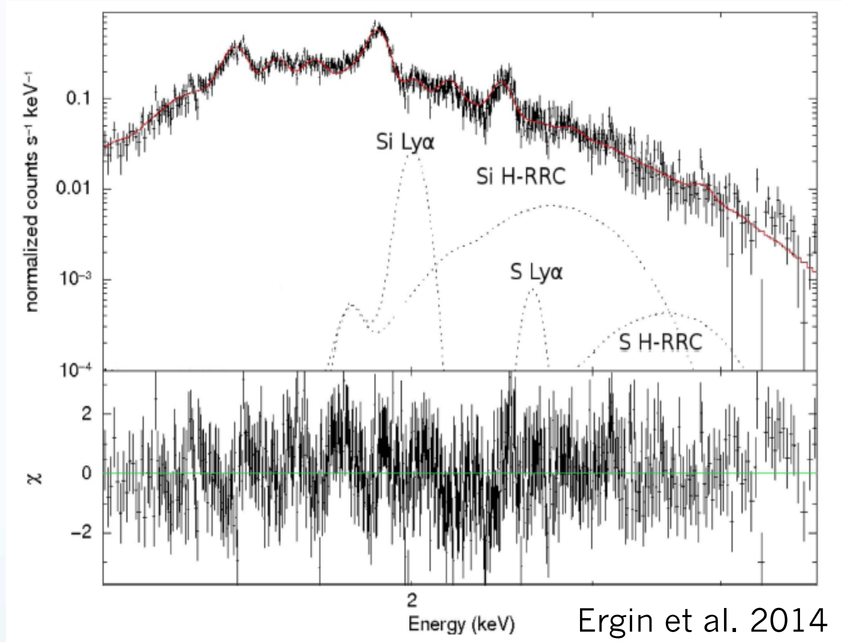

Ergin et al. 2014

X-ray Analysis Fit Results

Component	Parameters	Whole	NW	SE
wabs	N_H (10^{22} cm^{-2})	3.1 ± 0.1	3.4 ± 0.1	2.9 ± 0.1
VNEI	kT_e (keV)	0.58 ± 0.01	0.61 ± 0.01	0.54 ± 0.01
	Mg (solar)	1.2 ± 0.1	1.6 ± 0.2	1.4 ± 0.1
	Si (solar)	0.9 ± 0.1	0.9 ± 0.1	1.1 ± 0.1
	S (solar)	0.8 ± 0.1	0.7 ± 0.1	0.8 ± 0.1
	τ (10^{12} cm^{-3} s)	1.8 ± 0.2	1.7 ± 0.3	1.8 ± 0.1
	Norm (photon cm^{-2} s^{-1})	4.1 ± 0.4	3.1 ± 0.5	3.2 ± 0.9
Al Kα	E (keV)	1.58 (fixed)	1.58 (fixed)	1.58 (fixed)
	σ (keV)	0 (fixed)	0 (fixed)	0 (fixed)
	Norm (10^{-4}photon cm^{-2} s^{-1})	2.1 ± 0.2	2.2 ± 0.4	2.1 ± 0.1
Si Lyα	E (keV)	2.0 (fixed)	2.0 (fixed)	2.0 (fixed)
	σ (keV)	0 (fixed)	0 (fixed)	0 (fixed)
	Norm (10^{-4}photon cm^{-2} s^{-1})	4.9 ± 0.5	3.8 ± 0.3	3.9 ± 0.2
S Lyα	E (keV)	2.6 (fixed)	2.6 (fixed)	2.6 (fixed)
	σ (keV)	0 (fixed)	0 (fixed)	0 (fixed)
	Norm (10^{-4}photon cm^{-2} s^{-1})	3.6 ± 0.2	3.1 ± 0.3	2.9 ± 0.2
RRC H-like Si	E (keV)	2.666 (fixed)	2.666 (fixed)	2.666 (fixed)
	Norm (10^{-4}photon cm^{-2} s^{-1})	5.2 ± 0.3	4.3 ± 0.6	4.1 ± 0.3
RRC H-like S	E (keV)	3.482 (fixed)	3.482 (fixed)	3.482 (fixed)
	Norm (10^{-4}photon cm^{-2} s^{-1})	4.4 ± 0.5	3.7 ± 0.4	3.6 ± 0.2
Ergin et al. 2014	χ^2/dof	$860/717 = 1.2$	$452/361.6 = 1.25$	$301/251 = 1.2$

X-ray Analysis Fit Results

- Compared the kTe values of these regions
  - kTe for NW to be ~0.61 keV
  - kTe for SE region ~0.54 keV
- Since these values are very close to each other, it is not possible to determine which cooling mechanism is dominant.
- The age of 3C 391 as Trec ~ 69,000 yr using the best-fit τ value of VNEI+RP model.
- Tsnr ~40,000 yr from Chandra data.
- Since Trec < Tsnr, the electron cooling might have happened through adiabatic cooling.

Possible Scenarios to Explain the RP in 3C 391

- The break out scenario of 3C 391:
  - The massive progenitor star of 3C 391 inside an MC exploded and the shock waves expanded in the dense MC breaking out into a more rarefied ISM in the SW region
- The possible origin of the RP in the NW region might be due to the hot electrons getting in contact with cooler and denser MC impeding the expansion of the SNR shell.
- In the SE region, it is possible that the RP formed when SN blast wave expanded into the rarefied ISM and caused the electron temperature to drop through the adiabatic cooling mechanism.
- Or both of these cooling mechanisms might have worked together in different regions of the SNR to produce the overall drop in electron temperatures that we observed across the entire SNR.
  - To understand which scenario dominates in which part of 3C 391, detailed overionization maps need to be produced, as it is done for W49B (Lopez et al. 2013).

Other MM-SNRs Interacting With MC

Hadronic gamma rays from G349.7+0.2 detected but no RRC detection!

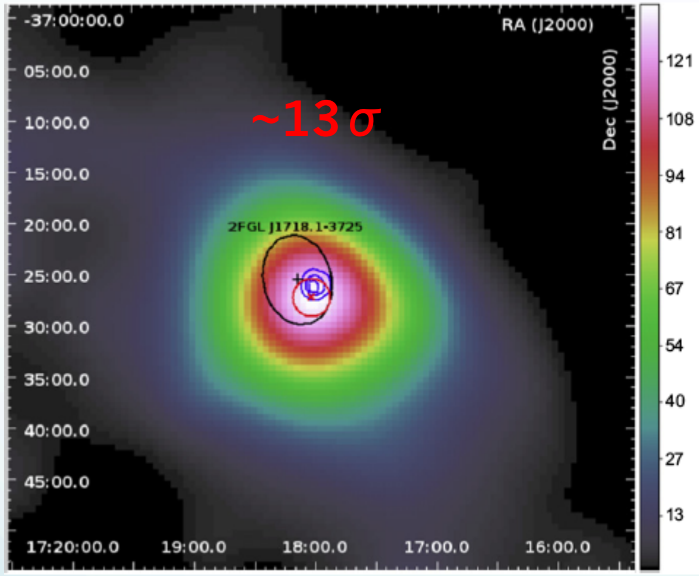

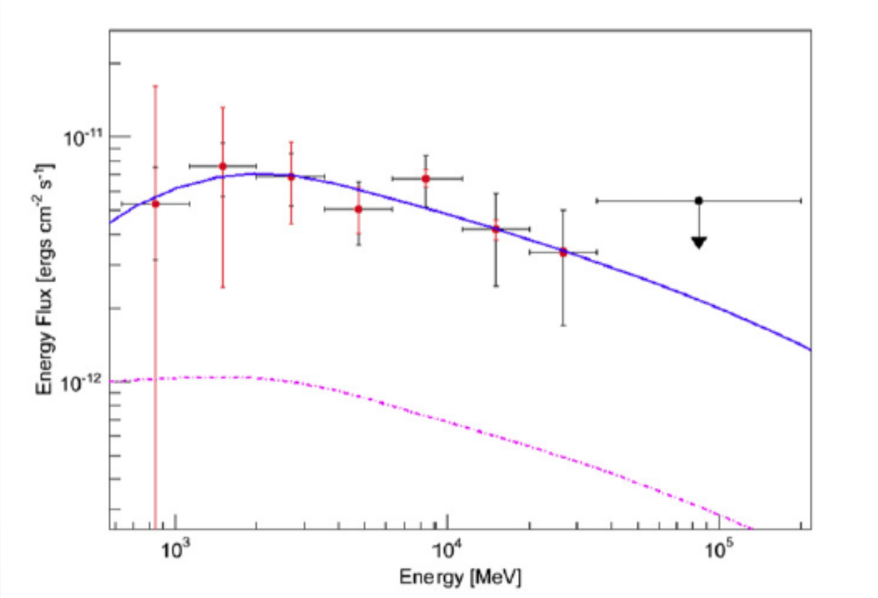

Ergin, T., Sezer, A., Saha, L., Majumdar, P., Gök, F., Bayirli, A., Ercan, E. N. (2015), Astrophysical Journal, 804, 124.

Conclusion

- Gamma rays gives an opportunity to study the acceleration processes of high-energy particles inside astrophysical sources, such as SNRs.
- Multi-wavelength data from the young shell-like Cas A was analyzed to determine a more precise location of TeV and GeV gamma rays inside Cas A.
  - The multi-wavelength spectrum of Cas A can be best described by the lepto-hadronic emission model.
  - The TeV and GeV gamma-ray emission may dominantly come from the southern region of Cas A's shell.
- We have studied the gamma-ray and X-ray emission the middle-aged MM-type SNR 3C 391
  - Modeling the spectrum revealed gamma-ray emission that can be explained by the hadronic emission model.
  - X-ray analysis revealed recombining plasma. Result compatible both with the thermal conduction and the break-out scenarios.
- Other MM-type SNR G349.7+0.2 interacting with MC was searched for hadronic emission & RP in X-rays. Gamma-ray spectrum showed hadronic emission but no RP.

41. COSPAR Scientific Assembly

- Turkey is a member of COSPAR since 1996.
- The 41st COSPAR Scientific Assembly will be held in Istanbul
- Date: 30 July – 7 August 2016
- Around 3000 participants from 60 countries are expected.
- Abstract submission Deadline:
  12 February 2016
- Early Registration Deadline:
  31 May 2016

Abstract Submission Page:
http://cosparhq.cnes.fr/
Local Organizing Committe's Page:
http://cospar2016.tubitak.gov.tr/